Received: 1 September 2023 | Revised: 8 November 2023 | Accepted: 8 December 2023

DOI: 10.1002/mp.16899

RESEARCH ARTICLE

MEDICAL PHYSICS

Dosimetrically motivated beam-angle optimization for non-coplanar arc radiotherapy with and without dynamic collimator rotation

Jenny Bertholet[1] | **Chengchen Zhu**[1] | **Gian Guyer**[1] | **Silvan Mueller**[1] | **Werner Volken**[1] | **Paul-Henry Mackeprang**[1] | **Hannes A. Loebner**[1] | **Marco F. M. Stampanoni**[2] | **Daniel M. Aebersold**[1] | **Michael K. Fix**[1] | **Peter Manser**[1]

[1]Division of Medical Radiation Physics and Department of Radiation Oncology, Inselspital, Bern University Hospital, and University of Bern, Bern, Switzerland

[2]Institute for Biomedical Engineering, ETH Zürich and PSI, Villigen, Switzerland

Correspondence
Jenny Bertholet, Division of Medical Radiation Physics and Department of Radiation Oncology, Inselspital, Freiburgstrasse, 3010 Bern, Switzerland.
Email: jenny.bertholet@extern.insel.ch

Funding information
Swiss National Science Foundation, Grant/Award Number: 200021_185366; Varian, a Siemens Healthineers Company

Abstract

Background: Non-coplanar techniques have shown to improve the achievable dose distribution compared to standard coplanar techniques for multiple treatment sites but finding optimal beam directions is challenging. Dynamic collimator trajectory radiotherapy (colli-DTRT) is a new intensity modulated radiotherapy technique that uses non-coplanar partial arcs and dynamic collimator rotation.

Purpose: To solve the beam angle optimization (BAO) problem for colli-DTRT and non-coplanar VMAT (NC-VMAT) by determining the table-angle and the gantry-angle ranges of the partial arcs through iterative 4π fluence map optimization (FMO) and beam direction elimination.

Methods: BAO considers all available beam directions sampled on a gantry-table map with the collimator angle aligned to the superior-inferior axis (colli-DTRT) or static (NC-VMAT). First, FMO is performed, and beam directions are scored based on their contributions to the objective function. The map is thresholded to remove the least contributing beam directions, and arc candidates are formed by adjacent beam directions with the same table angle. Next, FMO and arc candidate trimming, based on objective function penalty score, is performed iteratively until a desired total gantry angle range is reached. Direct aperture optimization on the final set of colli-DTRT or NC-VMAT arcs generates deliverable plans. colli-DTRT and NC-VMAT plans were created for seven clinically-motivated cases with targets in the head and neck (two cases), brain, esophagus, lung, breast, and prostate. colli-DTRT and NC-VMAT were compared to coplanar VMAT plans as well as to class-solution non-coplanar VMAT plans for the brain and head and neck cases. Dosimetric validation was performed for one colli-DTRT (head and neck) and one NC-VMAT (breast) plan using film measurements.

Results: Target coverage and conformity was similar for all techniques. colli-DTRT and NC-VMAT plans had improved dosimetric performance compared to coplanar VMAT for all treatment sites except prostate where all techniques were equivalent. For the head and neck and brain cases, mean dose reduction—in percentage of the prescription dose—to parallel organs was on average 0.7% (colli-DTRT), 0.8% (NC-VMAT) and 0.4% (class-solution) compared to VMAT.

The reduction in $D_{2\%}$ for the serial organs was on average 1.7% (colli-DTRT), 2.0% (NC-VMAT) and 0.9% (class-solution). For the esophagus, lung, and breast cases, mean dose reduction to parallel organs was on average 0.2% (colli-DTRT) and 0.3% (NC-VMAT) compared to VMAT. The reduction in $D_{2\%}$ for the serial organs was on average 1.3% (colli-DTRT) and 0.9% (NC-VMAT). Estimated delivery times for colli-DTRT and NC-VMAT were below 4 min for a full gantry angle range of 720°, including transitions between arcs, except for the brain case where multiple arcs covered the whole table angle range. These times are in the same order as the class-solution for the head and neck and brain cases. Total optimization times were 25%–107% longer for colli-DTRT, including BAO, compared to VMAT.

Conclusions: We successfully developed dosimetrically motivated BAO for colli-DTRT and NC-VMAT treatment planning. colli-DTRT and NC-VMAT are applicable to multiple treatment sites, including body sites, with beneficial or equivalent dosimetric performances compared to coplanar VMAT and reasonable delivery times.

KEYWORDS
beam angle optimization, dynamic trajectory radiotherapy, non-coplanar radiotherapy

1 | INTRODUCTION

Beam angle optimization (BAO) in radiation therapy has been the subject of extensive investigation for many years.[1] Nevertheless, current state-of-the-art techniques like coplanar intensity modulated radiation therapy (IMRT) and volumetric modulated arc therapy (VMAT) rely on treatment site-specific class-solutions and planner experience rather than BAO for beam/arc setup.[2] On the other hand, there has been a renewed interest for non-coplanar radiotherapy because planning studies have shown improved dosimetric plan quality for multiple treatment sites compared to standard coplanar techniques.[3–9] Non-coplanar beam arrangements exploit a greater number of possible beam directions which also increase the complexity of the BAO problem.

Several studies have proposed dosimetrically motivated BAO for non-coplanar 4π-IMRT.[10–12] However, despite positive results from a prospective trial for glioma patients in 2018,[13] 4π-IMRT has not yet found widespread clinical implementation. HyperArc, a class-solution non-coplanar VMAT (NC-VMAT), is commonly used for the treatment of brain metastases,[14] possibly owing to the more efficient dynamic delivery compared to 4π-IMRT. HyperArc was also recently applied to targets in the head and neck region.[15,16] Although such a class-solution already offers substantial freedom for intensity modulation optimization, not all potentially advantageous beam directions are considered for specific patients and there is increased risk of collision for target outside the skull-base.

Wild et al. have used optimization of multiple NC-VMAT arcs to solve the BAO problem for nasopharyngeal cases but restricted the search to +/−30° table angle to avoid collisions.[4] MacDonald et al. have automatically determined table angles and gantry-angle range for non-coplanar partial arcs with optimized collimator angle using overlap metrics to solve the BAO problem.[3] By considering partial arcs, the technique is more easily applicable to treatment sites in the body[17] where collision risk strongly limits the range of usable table angles for a full gantry rotation.

We previously used a similar overlap metric in a study for seven typical head and neck cases where table angles and gantry-angle ranges were determined from contoured structures by minimizing relative target/organ-at-risk (OAR) overlap in beam's eye view.[18] In this case, NC-VMAT was also extended to include dynamic collimator rotation during delivery, a technique we call dynamic-collimator trajectory radiotherapy (colli-DTRT). The dynamic collimator rotation was determined by minimizing the range of possible leaf travel for the chosen gantry-table paths.

However, by not considering the dosimetric interplay between different beam directions during BAO, these geometric methods[3,17,18] may result in suboptimal beam angle selection.

In this study, we solve the BAO problem with a dosimetrically motivated approach for colli-DTRT and NC-VMAT by determining the table angles and gantry-angle ranges of the partial arcs through iterative 4π-fluence map optimization (FMO) and beam direction elimination. colli-DTRT and NC-VMAT treatment plans with dosimetrically motivated BAO are created for a range of treatment sites and compared to state-of-the-art VMAT plans and class-solution non-coplanar VMAT plans where applicable.

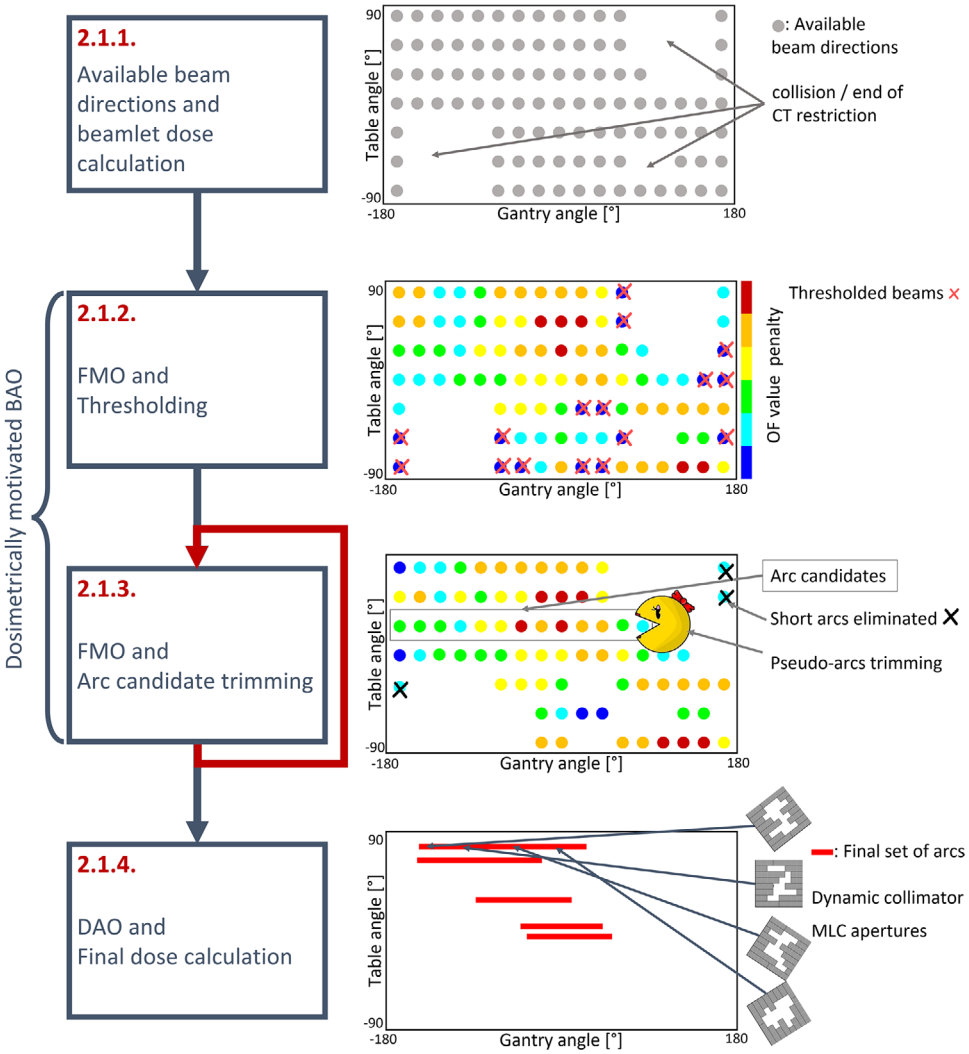

FIGURE 1 Left: treatment planning process for colli-DTRT. Individual steps are explained in the corresponding sections and illustrated on the right panel. Each dot on the map corresponds to an available beam direction with its color indicating the penalty on the overall objective function (OF) associated with removing this point from the pool of candidates.

2 | METHODS

2.1 | Treatment planning process for colli-DTRT

The main steps of the colli-DTRT treatment planning process are illustrated in Figure 1 and described in detail in the following.

2.1.1 | Available beam directions and beamlet dose calculation

First, the patient CT image set is imported into a research version of the Eclipse Treatment Planning System (TPS) v15.6 (Varian Medical Systems) and the planning target volume (PTV), OARs, and normal tissue (body excluding PTV) are contoured. An interface to the Swiss Monte Carlo Plan (SMCP) is used, with contours exported as triangular meshes.[19] For each possible beam direction defined by the gantry and table angle, called map point hereafter, the collimator angle is aligned to the patient's superior-inferior axis. This leads to subsequent dynamic collimator rotation for all arcs with table angle different from 0°. Because most non-spheroid tumors are elongated in the superior-inferior axis, such an alignment is expected to minimize potential leaf travel. A collision prediction tool using Blender, an open-source 3D computer graphics software toolset, considers the estimated absolute table position and a generic patient model to eliminate map points that can lead to a collision of the gantry with the table or the patient.[20] Map points where any beamlet, restricted to a conformal aperture around the target volume enlarged by a 5 mm margin, would enter through the end of the CT stack are also eliminated. Next, beamlet dose calculation is performed for each available map point using Voxel Monte Carlo (VMC++)[21] executed

within the SMCP framework with pre-simulated phase-spaces located at the treatment head exit plane as source.[22] The phase-space source was computed using the BEAMnrc package, for a mean energy matched to measured dose distributions; it was scored directly above the secondary collimator jaw, perpendicular to the beam central axis.

In this work, map points were sampled every 10° gantry angle from −180° to +180° and every 10° table angle from −90° to +90°. Beamlet size at isocenter was 5×5 mm^2 for inner 5 mm leaves or 5×10 mm^2 for outer 10 mm thick leaves for a Millennium 120 multi-leaf collimator (MLC) (Varian) and beamlet doses were calculated using a $5 \times 5 \times 5$ mm^3 voxel size for the BAO steps (Sections 2.1.2 and 2.1.3).

2.1.2 | FMO and thresholding

Next, FMO is performed for the available map points using a limited-memory Broyden-Fletcher-Goldfarb-Shanno (L-BFGS) algorithm to minimize the objective function which quadratically penalizes deviations of the dose distribution from upper and lower dose-volume objectives, generalized equivalent uniform dose, and normal tissue objectives with their associated weights.[23] After FMO, a penalty score based on objective function value is calculated for each map point as follows: consider $F(D)$, the objective function value for the dose distribution optimized on all the map points. $F(D'_{-mp_i})$ denotes the objective function value when ignoring the contribution of map point i, mp_i, to the dose distribution. The penalty score for mp_i is calculated as $Q_{mp_i} = \frac{1}{F(D)}[F(D'_{-mp_i}) - F(D)]$. This is motivated by the following assumption: the greater the importance of a map point, the greater the increase of the objective function value when removing its contribution, hence the greater the penalty in eliminating this map point.

The penalty score map is then thresholded, removing low score map points. Arc candidates are formed by remaining adjacent map points with the same table angle.

2.1.3 | Iterative FMO and arc candidate trimming

After one thresholding, FMO is repeated for the remaining map points and the penalty score map is recalculated. Arc candidates are trimmed by removing up to a given percentage of low-score map points as in Section 2.1.2. For trimming, contrary to thresholding, arc connectedness is preserved by only allowing elimination of map points at the arc candidate edges. During each trimming step, map points are eliminated one by one, that is, after the lowest score map point is removed, the adjacent map point becomes an edge and is therefore eliminable. FMO and trimming are repeated iteratively until a user-defined total gantry-angle range is reached. If several map points have the same value (with float precision), only one is eliminated so as not to eliminate more points than requested.

In this work, given that FMO was used only for BAO and not for final treatment plan optimization, L-BFGS was terminated if the objective function value was not lowered more than 10% in three consecutive iterations. For the thresholding (Section 2.1.2) and each following trimming iteration (Section 2.1.3), we eliminated 25% of the map points with the lowest score. We also applied a small-arc rejection criterion where arc candidates spanning less than 30° gantry-angle were eliminated after thresholding and during trimming. This corresponds to the minimum arc length that can be optimized using the VMAT photon optimizer in Eclipse and prevents from having colli-DTRT plans with many very small arcs or single fields. Because of this, the final total gantry angle range could be up to 20° (30° minimum arc length criterion minus 10° gantry angle sampling) shorter than the user-defined total gantry-angle range.

2.1.4 | DAO and final dose calculation

The final set of arc candidates are then considered as dynamic arcs and subjected to intensity modulation optimization using a hybrid-direct aperture optimization (DAO) combining column generation and simulated annealing.[23,24] Final dose calculation of the optimized apertures is performed in SMCP using VMC++ to simulate the plan-specific part of the treatment head including the secondary collimator jaws and MLC and to calculate dose deposition in the patient, accounting for the continuous motion of all dynamic components between the discrete control points (CP). Finally, monitor unit (MU) weights are re-optimized using a L-BFGS algorithm.

In this work, a relatively coarse grid with map points every 10° gantry angle and a large voxel size of $5 \times 5 \times 5$ mm^3 were used for the BAO steps to reduce beamlet dose calculation time and memory usage as well as BAO optimization times. Hence, the arcs were resampled prior to DAO with CP every 5° gantry-angle and beamlet doses were calculated using a $2.5 \times 2.5 \times 2.5$ mm^3 voxel size with the same beamlet grid resolution as in Section 2.1.1.

2.2 | Investigated cases and analysis

colli-DTRT and NC-VMAT plans were created for seven clinically motivated cases described in Table 1. For NC-VMAT, the collimator alignment step at Section 2.1.1. is omitted, instead the collimator angle remained static at

TABLE 1 Clinically motivated cases included in this study with coplanar VMAT and class-solution arc set-up.

Case	Indication	Prescription	VMAT geometry	Class solution geometry
1	Head and neck—Adenoid cystic carcinoma (elective volume)	25 x 2 Gy (95% of the PTV)	2 full arcs, colli 2° and 88°	1 full arc, colli 162°, table 0° 1 arc 180-0°, colli 66°, table 270° 1 arc 0-180°, colli 69°, table 45°
2	Head and neck—unilateral elective nodal volume	25 x 2 Gy (95% of the PTV)	2 full arcs, colli 2° and 88°	1 full arc, colli 359°, table 0° 1 arc 0-180°, colli 347°, table 315° 1 arc 180-0°, colli 123°, table 270°
3	Brain—Glioblastoma	30 x 2 Gy (median PTV volume)	2 full arcs, colli 2° and 88°, table 0°	1 full arc, colli 147°, table 0° 1 arc 180-0°, colli 69°, table 45° 1 arc 0-180°, colli 102°, table 315° 1 arc 180-0°, colli 51°, table 270°
4	Esophagus	25 x 1.8 Gy (median PTV volume)	2 full arcs, colli 2° and 88°	NA
5	Lung—locally-advanced non-small cell lung cancer	33 x 2 Gy (median PTV volume)	2 full arcs, colli 2° and 88°	NA
6	Breast—whole breast irradiation	16 x 2.65 Gy (median PTV volume)	3 partial arcs 290-179°, colli 2°, 2° and 88°	NA
7	Prostate	40 x 2 Gy (median PTV volume)	2 full arcs, colli 2° and 88°	NA

Note: For cases 1 and 2, the partial arcs at table angle 45° and 315° respectively were omitted due to collision risk.
For case 6, full arcs were not possible due to collision risk, the total gantry-angle range remains 720°.

2°. colli-DTRT and NC-VMAT plans were compared to coplanar VMAT plans using the same total gantry-angle range of 720°. For cases in the brain or head and neck, class-solution non-coplanar plans were created using the arc set-up of HyperArc with fixed collimator angles.

All plans were created for a TrueBeam delivery system equipped with a Millennium 120 MLC (Varian) for 6 MV flattened photon beams. All plans were optimized using the same optimizer, CP spacing, and voxel grid as described in Section 2.1.4. The same list of optimization objectives was used for all the plans for each given case.

Plans were compared based on objective function value and dosimetric endpoints after final SMCP dose calculation. Delivery time was estimated for each plan based on maximum speed of the linac components, including the time needed for gantry, table, and collimator rotation between arcs. Beamlet dose calculation (parallelized) and optimization times[22,23] for the BAO and DAO steps were reported. Dose calculations and optimizations were performed on a single Intel Broadwell CPU with 2 × 10 cores.

2.3 | Deliverability in research and clinical mode

A verification plan was created for the colli-DTRT plan of case 1 for a polymethyl methacrylate (PMMA) cubic phantom[25] and exported in extended markup language (xml) format. The plan was delivered on a TrueBeam using Developer Mode on the phantom with 2 interleaved EBT3 films (Ashland Advanced Materials, Bridgewater, NJ) for the sagittal and coronal planes. The films were scanned 18 h after irradiation on an Epson XL 10000 flatbed scanner and corrected for lateral response artefact using a one-dimensional linear correction function.[26] Triple channel calibration was used to convert color values to absolute dose[27] and dose was rescaled according to the one-scan protocol.[28] The resulting dose to the red channel was used for comparison with the corresponding SMCP-calculated dose planes using gamma evaluation with a 3% (global)/2 mm criterion and a 10% dose threshold of the maximum dose following AAPM recommendation.[29,30]

colli-DTRT plans cannot be optimized using clinical algorithms or delivered in clinical mode due to the dynamic collimator rotation; but NC-VMAT plans can. To demonstrate feasibility, we imported the NC-VMAT paths determined using the dosimetrically motivated BAO for case 6 into the TPS, optimized the plan using the photon optimizer and calculated the final dose using the analytical anisotropic algorithm (AAA). A verification plan was created for the cubic phantom and exported in DICOM format to be delivered in clinical mode on a TrueBeam for film measurement as described above. The measured dose was compared to the AAA-calculated dose.

3 | RESULTS

All generated plans were reviewed by a radiation oncologist and found to be clinically acceptable.

3.1 | Head and neck cases

Table 2 reports the OAR dosimetric endpoints and estimated delivery time for all techniques for the head and

TABLE 2 Dosimetric endpoints and estimated delivery times for the head and neck cases. The best value for each endpoint is indicated in bold.

Endpoint (in Gy unless specified otherwise)	colli-DTRT	NC-VMAT	VMAT	Class-solution
Case 1 - Head and neck—Adenoid cystic carcinoma (elective volume)				
Paddick CI [%]	89	89	89	89
PRV spinal cord $D_{2\%}$	21.4	21.6	**21.2**	**21.2**
PRV brainstem $D_{2\%}$	**12.6**	12.9	13.8	12.6
CL carotid $D_{10\%}$	**3.4**	3.9	5.9	5.1
CL carotid $D_{30\%}$	**2.9**	3.1	4.6	4.1
CL carotid $D_{50\%}$	**2.5**	**2.5**	3.8	3.5
CL parotid[1] D_{mean}	1.3	**0.8**	2.7	2.3
CL submand. D_{mean}	**2.1**	2.4	2.6	2.6
IL submand. D_{mean}	25.0	**24.8**	25.1	25.3
Oral cavity D_{mean}	5.5	**4.8**	7.1	6.5
Pharynx D_{mean}	9.0	**8.5**	8.8	8.8
Larynx D_{mean}	6.5	6.4	**3.7**	6.2
IL Cochlea $D_{2\%}$	22.7	25.7	**21.7**	23.0
Brain $D_{2\%}$	23.9	26.5	30.0	**23.8**
Delivery time [min]	3.1	3.0	**2.2**	3.1
Case 2 - Head and neck—unilateral elective nodal volume				
Paddick CI [%]	89	90	**92**	**92**
PRV spinal cord $D_{2\%}$	**25.8**	26.8	28.3	27.3
PRV brainstem $D_{2\%}$	**15.5**	15.7	15.9	16.2
CL carotid $D_{10\%}$	13.9	**13.2**	16.1	13.5
CL carotid $D_{30\%}$	9.4	**8.4**	10.1	9.4
CL carotid $D_{50\%}$	6.8	**5.8**	7.5	6.0
CL parotid D_{mean}	**4.9**	5.2	5.9	5.4
IL parotid D_{mean}	20.3	**20.1**	20.8	20.8
Oral cavity D_{mean}	20.6	**20.3**	21.3	20.5
Pharynx D_{mean}	33.5	**33.3**	33.7	**33.3**
Larynx D_{mean}	7.3	**6.7**	7.1	7.2
Lips D_{mean}	**7.7**	8.2	8.8	9.0
Lips $D_{2\%}$	**14.0**	15.6	15.9	15.6
Brain $D_{2\%}$	17.7	**15.4**	**15.4**	18.0
Delivery time [min]	2.5	3.2	**2.2**	3.3

Note: IL parotid was resected in case 1, IL + CL submand were resected in case 2.
Abbreviations: CI, conformity index; CL, contralateral; IL, ipsilateral; PRV, planning-at-risk volumes.

neck cases and Figure 2 shows selected dose volume histogram (DVH).

The details of the BAO process for colli-DTRT and NC-VMAT are illustrated in Figure 3 for case 1. The two techniques resulted in a different set of paths due to the difference in collimator angles. colli-DTRT had nine paths, after three trimming steps, with table angles between +50 and −70°; NC-VMAT had 10 paths with table angles between 60 and −70°.

The dose distribution for the four techniques in one axial plane are shown in Figure 4. colli-DTRT or NC-VMAT achieved better sparing than VMAT or the class-solution for most OARs (Table 2). VMAT achieved better sparing than all the non-coplanar techniques for the larynx and ipsilateral cochlea.

For case 2, colli-DTRT had seven arcs, after four trimming steps, with table angles between +70° and +10°, covering gantry angles between −160° and +30° while NC-VMAT had nine arcs with table angles between +70° and −30° covering gantry angles between −150° and +50°. colli-DTRT had better sparing than the other techniques for spinal cord and brainstem PRVs, contralateral parotid gland and lips. NC-VMAT had the best sparing for the other OAR endpoints.

3.2 | Brain case

Table 3 reports the dosimetric endpoints and estimated delivery time for the brain case and DVHs shown in Figure S1.

Here, note that colli-DTRT, NC-VMAT, and VMAT all had a total gantry angle range of 720° (i.e., 2 full arc-equivalent) while the class-solution had an additional half arc, totaling 900°. colli-DTRT had 17 arcs and NC-VMAT 12, after five trimming steps, both with table angles covering the whole range from −90° to +90°.

3.3 | Thorax cases

Table 4 reports the dosimetric endpoints and estimated delivery times for the thorax cases. All plans had Paddick CI of 50%.

Figure 5 shows the first optimization and the last BAO step, after two trimming steps, for case 4 (esophagus) for colli-DTRT and NC-VMAT as well as the DVHs for all three plans. Although the collision-free space is smaller compared to the head and neck and brain cases, the dosimetric BAO results in highly non-coplanar plans with colli-DTRT having 13 arcs with table angles between +50° and −40°; NC-VMAT had 12 arcs with table angles between +30° and −40°. Similar to case 1 (Figure 3) the different collimator angle results in a different beam direction selection.

Figure 6 shows the DVHs for case 5 (lung) and 6 (breast). For case 5, colli-DTRT had 11 arcs, after two trimming steps, with table angles between +50° and −30° and gantry angles ranging from −180° to 0°. NC-VMAT had five arcs with table angles between +20° and −20° and gantry angles ranging from −180° to +30°. For case 6, colli-DTRT had six arcs, after one trimming step, with table angles between +30° and-10°; NC-VMAT had seven arcs with table angles between +30° and −20°.

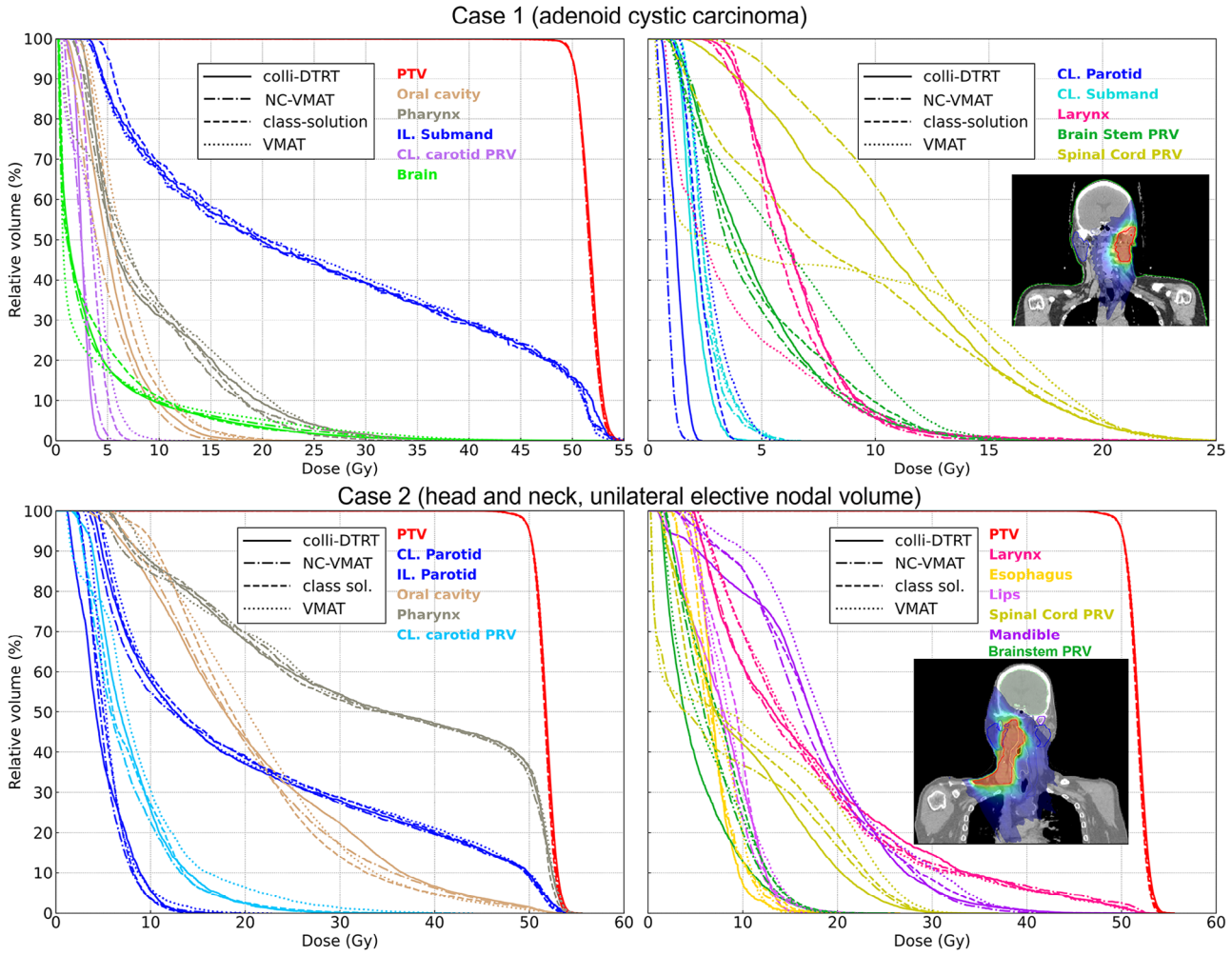

FIGURE 2 DVHs for the head and neck cases (1, top and 2, bottom). The inserts show a coronal view of the colli-DTRT dose distribution (color scale: 5%−109% of the prescription dose).

3.4 | Prostate case

For case 7 (prostate), colli-DTRT had seven arcs, after one trimming step, with table angles between +20° and −10°; NC-VMAT had nine arcs with table angles between +20° and −20°. DVHs are shown in Figure S2. All plans had similar target coverage and Paddick CI of 0.50. OAR endpoints (V_{50Gy}, V_{65Gy}, V_{70Gy} and V_{75Gy} to the rectum and rectum wall; V_{50Gy} and V_{70Gy} to the bladder and bladder wall) were similar for all techniques (data not shown). However, mean dose to the rectum, rectum wall, bladder, and bladder wall (not part of the optimization objectives) was reduced by 0.5 to 0.7 Gy with colli-DTRT compared to VMAT. For the femoral heads, NC-VMAT had a mean dose of 7.7 Gy (both left and right) whereas it was 6.2 and 6.6 Gy (colli-DTRT) and 6.2 and 5.9 Gy (VMAT). Estimated delivery times were 3.5 min (colli-DTRT), 3.8 min (NC-VMAT), and 2.3 min (VMAT).

3.5 | Normal tissue dose, objective function values, and optimization times

DVHs for the normal tissues are reported in Figures S3 and S4. Although the volumes receiving low doses are generally smaller for VMAT than the non-coplanar techniques, the volumes receiving intermediate doses are lower for the non-coplanar techniques than for VMAT. The objective function (OF) value after final dose calculation and MU weight re-optimization relative to the VMAT plan are shown in Figure 7 for all cases and generally reflect the dosimetric differences reported above. The reduction in OF value with non-coplanar techniques was greatest for the head and neck and brain cases with maximum reductions of 26% for colli-DTRT for case 1, 42% for NC-VMAT for case 2 and 31% for the class-solution for the brain case. The reduction in OF value with non-coplanar techniques was generally more modest in the thorax with reduction between 5% and 16%

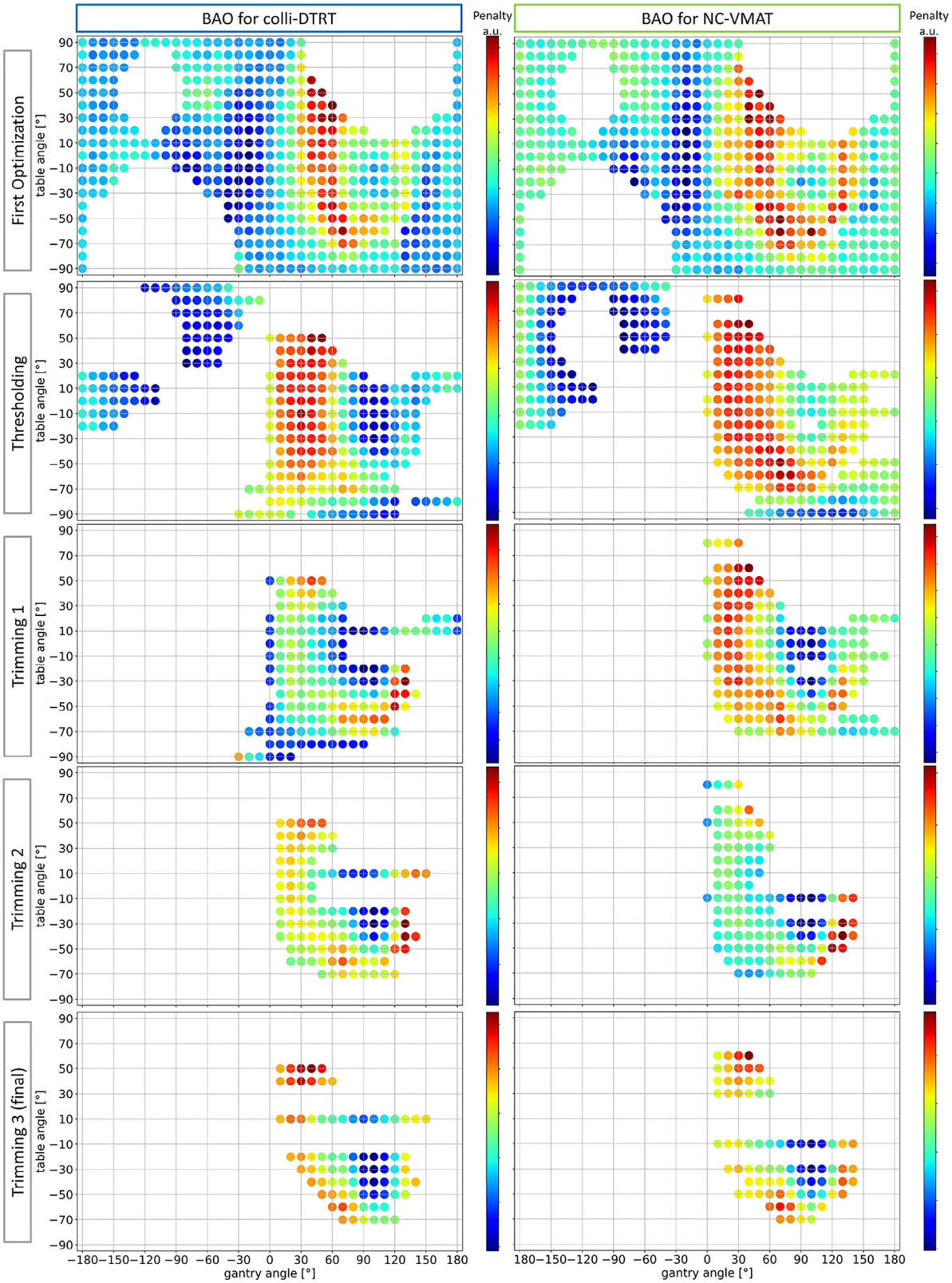

FIGURE 3 Score map (colorbar) for the BAO steps for colli-DTRT and NC-VMAT for case 1 (head and neck, adenoid cystic carcinoma). High scores (in red) correspond to a high penalty on the overall objective function associated with removing this point from the pool of candidates. The difference in collimator angle causes differences in contribution and hence in path selection.

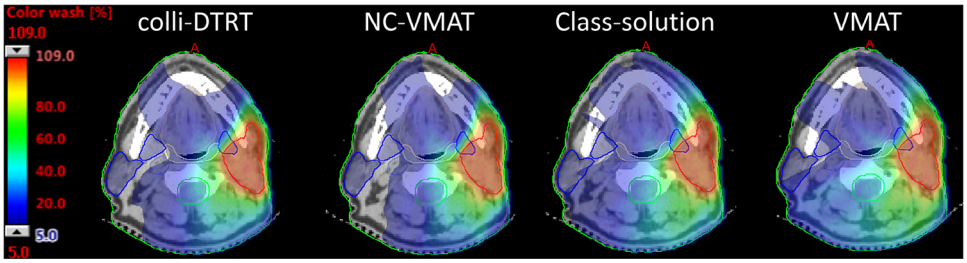

FIGURE 4 Dose distribution in a chosen axial slice for the four techniques. The PTV is shown in red, the parotid and submandibluar glands in blue, the oral cavity in beige, the pharynx in light beige, the carotid PRV in light purple, and the spinal cord in green.

TABLE 3 Dosimetric endpoints and estimated delivery times for the brain case.

Endpoint (in Gy unless specified otherwise)	colli-DTRT	NC-VMAT	VMAT	Class-solution
Brain—Glioblastoma				
Paddick CI [%][31]	**87**	85	85	**87**
Brain-PTV D_{mean}	**16.6**	17.0	18.5	18.2
Brain-PTV $D_{2\%}$	**53.8**	53.9	54.0	**53.8**
Brainstem $D_{2\%}$	44.9	42.7	42.2	**41.8**
Chiasm $D_{2\%}$	15.2	**14.3**	16.4	15.4
Optic nerve R $D_{2\%}$	7.3	**6.2**	8.0	7.5
Optic nerve L $D_{2\%}$	**4.9**	6.1	6.9	6.5
Lens R $D_{2\%}$	2.9	**2.1**	3.3	2.6
Lens L $D_{2\%}$	2.9	2.8	3.2	**2.4**
Lacr. gland R D_{mean}	**3.2**	**3.2**	3.4	3.4
Lacr. gland L D_{mean}	**2.6**	2.7	2.9	**2.6**
Eye R D_{mean}	3.5	**2.8**	4.0	3.5
Eye R $D_{2\%}$	5.3	**5.0**	6.9	5.9
Eye L D_{mean}	2.9	2.9	3.5	**2.8**
Eye L $D_{2\%}$	4.0	4.6	6.0	**3.7**
Delivery time [min]	4.9	3.9	**2.1**	3.5

Note: The best value for each endpoint is indicated in bold.
Abbreviations: CI, conformity index; L, left; R, right.

with colli-DTRT. For the prostate case, all techniques had similar OF within 1%.

Beamlet dose calculation and optimization times are summarized in Figure 8 for colli-DTRT and VMAT, and in Figure S5 for all techniques. The DAO times are similar between the techniques (except for the class solution in case 3 which had one additional half arc). For colli-DTRT and NC-VMAT, the map beamlet dose calculation (step 2.1.1 in Figure 1) was between 8.4 min for case 7 (prostate) with a small target volume and only 301 available map points due to the large restriction space; and up to 88.4 min for case 2 (head and neck) with a large target volume and 462 available map points. The time for BAO (Sections 2.1.2 and 2.1.3 in Figure 1) was between 2.5 min for case 7 and 33.4 min for case 2. The longest case to optimize was case 6 (breast) which took 3 h for VMAT and 4 h 13 min for colli-DTRT including BAO. Case 7 took a total of 29 min for VMAT and 36 min for colli-DTRT including BAO.

3.6 | Deliverability in developer and clinical mode

The colli-DTRT plan of case 1 was successfully delivered on a TrueBeam in Developer mode with gamma passing rates between the measured and SMCP-calculated dose of 99.6% (coronal film) and 97.3% (sagittal film).

For case 6, the NC-VMAT paths were successfully imported into Eclipse and the plan was optimized using the photon optimizer. The VMAT plan was also reoptimized in Eclipse for comparison as shown in Figure S6. NC-VMAT had better OAR sparing than VMAT for all endpoints except mean dose to the ipsilateral lung. The NC-VMAT plan was successfully delivered on a TrueBeam in clinical mode with gamma passing rates between the measured and AAA-calculated dose of 97.6% (coronal film) and 99.9% (sagittal film). Figure 9 shows the comparison between measured and calculated dose for the two experiments.

4 | DISCUSSION

In this work, we introduced dosimetrically motivated BAO for NC-VMAT and for colli-DTRT which delivers intensity modulated radiotherapy during dynamic gantry and collimator rotation with multiple non-coplanar partial arcs. Compared to state-of-the-art VMAT, colli-DTRT improved plan quality as measured by objective function value and dosimetric endpoints, except for a prostate case where colli-DTRT and VMAT were equivalent. The greatest improvements in terms of OF value reduction were observed for three cases in the head and neck and the brain where there is large collision-free space. Nevertheless, because relatively small partial arcs were allowed, BAO also resulted in highly non-coplanar beam arrangements in the thorax. For the prostate case, the BAO solution was close to coplanar arcs and plan quality was similar to VMAT, indicating that coplanar geometry

TABLE 4 Dosimetric endpoints and estimated delivery times for the thorax cases.

Endpoint (in Gy unless specified otherwise)	colli-DTRT	NC-VMAT	VMAT
Esophagus			
Lung L D_{mean}	**11.0**	11.2	11.4
Lung R D_{mean}	10.1	**9.9**	**9.9**
Lung total D_{mean}	10.6	**10.5**	10.6
Lung total V_{20Gy} [%]	**14.2**	15.6	16.0
Heart D_{mean}	**24.4**	**24.4**	24.8
Liver D_{mean}	14.3	**14.2**	15.6
Liver V_{30Gy} [%]	9.8	10.0	**9.7**
Kidney L $D_{mean}/D_{2\%}$	**3.9/21.2**	4.2/21.7	4.8/24.3
Kidney R $D_{mean}/D_{2\%}$	**3.4/10.7**	3.8/12.7	4.3/14.3
Spinal canal $D_{2\%}$	**18.2**	22.3	26.6
Bowel $D_{2\%}$	45.5	**45.0**	45.7
Delivery time [min]	3.6	3.5	**2.1**
Lung—primary non-small cell lung cancer			
PRV spinal cord $D_{2\%}$	**15.6**	15.8	17.1
Lung IL D_{mean}	19.3	**19.2**	19.4
Lung IL V20Gy	**40.6**	40.7	41.7
Lung CL D_{mean}	**4.2**	4.3	5.0
Lung Total D_{mean}	**12.1**	**12.1**	12.6
Lung total V_{20Gy} [%]	**21.3**	21.6	22.0
Heart D_{mean}	**4.8**	**4.8**	5.2
Heart V_{20Gy} [%]	**4.4**	**4.4**	5.9
Esophagus D_{mean}	8.9	**8.8**	9.0
Delivery time [min]	3.7	2.9	**2.2**
Breast—whole breast irradiation			
Lung L D_{mean}	**9.5**	**9.5**	**9.5**
Lung L V_{16Gy} [%]	**18.9**	19.4	19.1
LungL $V5_{Gy}$ [%]	56.1	**52.9**	56.1
Lung R D_{mean}	1.9	**1.7**	2.7
Lung total D_{mean}	**5.6**	**5.6**	6.1
Lung total V_{5Gy} [%]	28.0	**26.1**	32.0
Heart D_{mean}	3.9	**3.7**	4.6
Heart V_{10Gy} [%]	2.7	**2.5**	5.1
CL breast D_{mean}	2.8	**2.6**	3.8
CL breast $D_{5\%}$	8.4	**7.7**	8.3
Spinal canal $D_{2\%}$	6.4	**5.9**	6.2
Delivery time [min]	2.8	3.3	**2.3**

Note: The best value for each endpoint is indicated in bold.

may be optimal for this indication. More marked improvements were seen in the thorax, where tangential beam directions can improve OAR sparing at depth. Further investigations in larger cohorts should be conducted to conclude on the benefits of dosimetrically motivated BAO for non-coplanar techniques in these indications.

colli-DTRT with dosimetrically motivated BAO is applicable to all treatment sites, unlike commercially available class-solutions like HyperArc with its use limited to brain[14] and some head and neck cases.[15,16] In this study we also considered class-solution non-coplanar plans for the three cases in the brain and head and neck. For the brain case, the class-solution had the lowest overall objective function, but it had a greater total gantry angle range than the other techniques, potentially offering more freedom to the optimizer during DAO. Despite a shorter total gantry angle range, the estimated delivery time was longer for colli-DTRT than the class-solution because colli-DTRT had multiple short arcs covering the entire range of possible table angles and the table speed is limited to 3°/s, twice as slow as the gantry. For head and neck cases treated with non-coplanar techniques, the optical structures and the bilateral hippocampus could be on the beam path and receive higher doses than with VMAT.[9] These structures were not contoured in the clinical structure sets, but they should be considered in future planning comparisons.

For four cases, NC-VMAT provided the best plans. This technique was investigated as an alternative to colli-DTRT where the collimator is static for each partial arc but BAO is dosimetrically motivated. This might indicate that non-coplanarity and dosimetrically motivated BAO were the main contributor to improved plan quality rather than dynamic collimator rotation. Even in the brain and head and neck, where class-solutions have been shown to be beneficial over VMAT,[14–16] NC-VMAT and colli-DTRT may offer further dosimetric improvements with dosimetrically motivated BAO.

In case 2, the target is elongated, approximately aligned with the superior-inferior axis of the patient. It was expected that maintaining the collimator aligned with the patient's superior-inferior direction for colli-DTRT would facilitate DAO by minimizing the range of potential leaf travel. In NC-VMAT, the paths found during BAO were different than for colli-DTRT and upon inspection of the optimized aperture shapes, it is clear that BAO for NC-VMAT chose beam directions where potential leaf travel is short. For colli-DTRT the actual main axis of the target appears to be slightly tilted with respect to the superior-inferior axis. The BAO process is therefore influenced by the collimator angle chosen a priori and further investigations on the most suited collimator alignment strategies are required to better exploit the potential benefits of dynamic collimator rotation.

Another possible improvement of the method would be to use DAO instead of FMO at the BAO step for simultaneous beam-angle and intensity modulation optimization. Although the dosimetrically motivated BAO is an improvement over geometric criteria,[18] it still neglects many restrictions in the delivery. Instead of eliminating beam directions based on FMO, a promising approach would be to determine anchor points and "grow" the

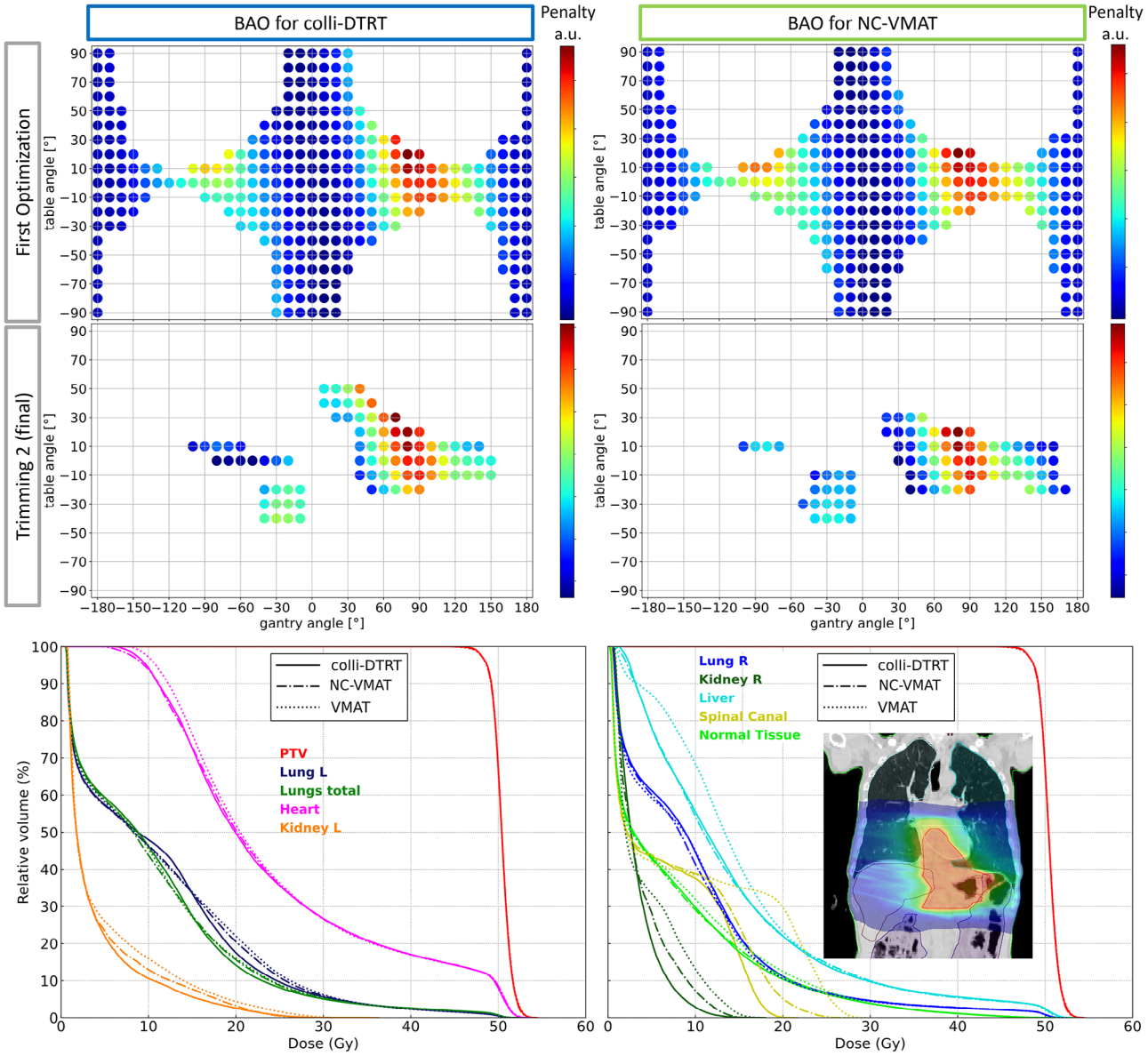

FIGURE 5 For case 4 (esophagus), score map at the first optimization and the last trimming step (2nd trimming) for colli-DTRT (top left) and NC-VMAT (top right) and the DVHs for all plans (bottom). The insert in the DVH shows a coronal view of the colli-DTRT dose distribution (color scale: 5%−109% of the prescription dose).

arcs by adding apertures at the candidate arc edges using a column generation algorithm.[7,11,12] Growing from anchor points could be further generalized to dynamic table rotation by allowing the addition of new beam directions at adjacent table angle. Lyu et al. also proposed to iterate between simultaneous BAO/DAO and path-finding to optimize treatment plans where the table rotates across the entire available range and the gantry is allowed to rotate back and forth. However, in the current implementation, continuous motion of the dynamic component between different beam directions is neglected.[32]

In this study, the same optimization objectives were used for all techniques, without any changes of priorities during the optimization process. This enables plan comparison based on one number: the objective function value. Optimization objectives were found empirically and adjusted so that, for each technique, target coverage was acceptable and all OARs had some contribution to the objective function value, at least at the BAO stage. Even better results could be obtained by tailoring the planning objectives for each technique and between the BAO and DAO stages for colli-DTRT and NC-VMAT. In particular for colli-DTRT and NC-VMAT, sparing of certain OARs could be further prioritized already at the BAO stage by increasing the priority of the objectives.

Although VMAT remains the fastest technique, colli-DTRT and NC-VMAT had estimated delivery times

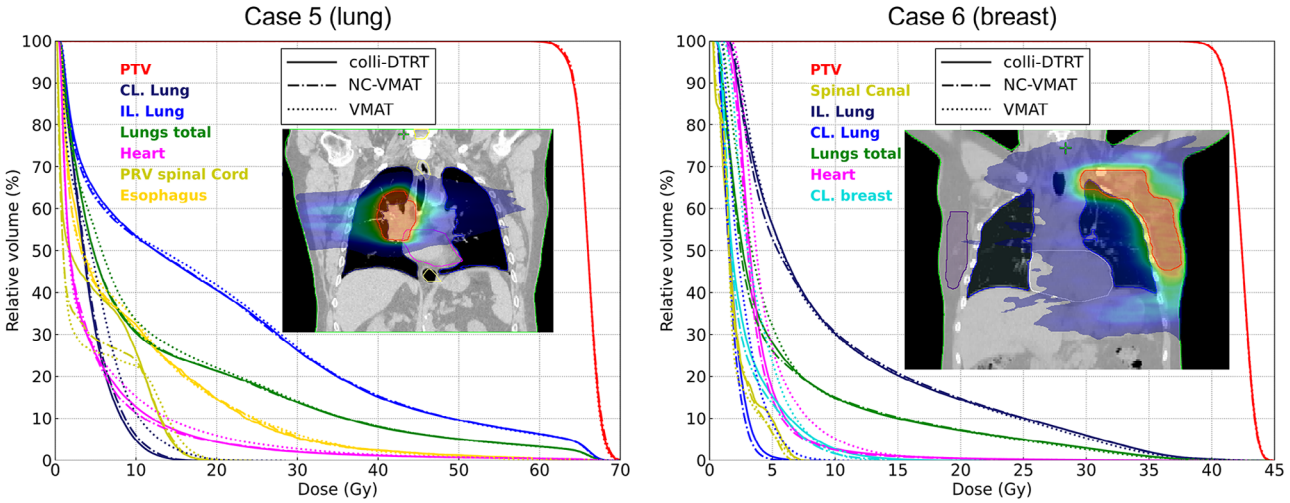

FIGURE 6 DVHs for case 5 (lung, left) and case 6 (breast, right). The inserts show a coronal view of the colli-DTRT dose distribution (color scale: 5%–109% of the prescription dose).

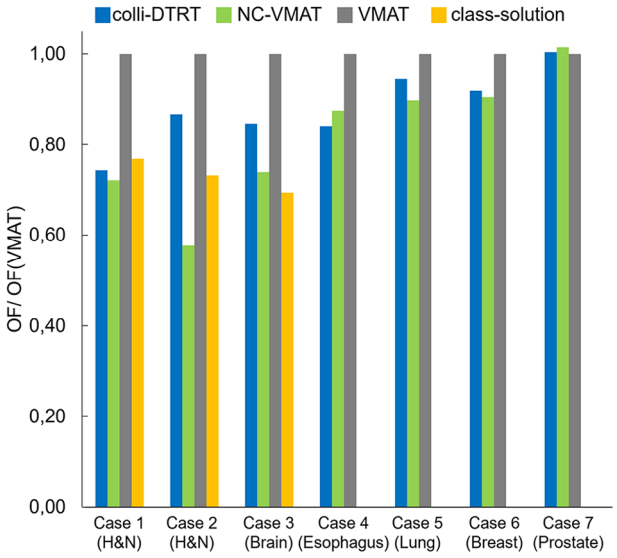

FIGURE 7 Objective function value relative to the VMAT plan for all investigated cases. The class solution is only applicable to the brain and head and neck cases.

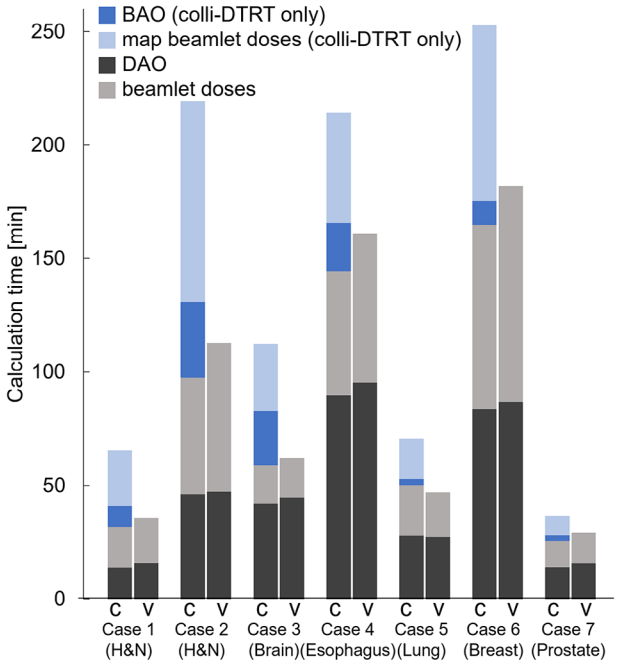

FIGURE 8 Beamlet dose calculation and optimization times for colli-DTRT (denoted with a c) and VMAT (v).

below 4 min, including transitions between arcs, except for the brain case where there were multiple arcs covering the whole table-angle range. These times are in the same order as the class-solution for the head and neck and brain cases. Delivery efficiency was not the focus of the present study but this could be considered in further improvements of the optimization process or indirectly by increasing the minimum arc length criterion.

In terms of optimization times, dosimetrically motivated BAO requires time for beamlet dose calculation for all available map points and for the iterative FMO and elimination process. This time varied between cases, depending on target size and the number of available map points. However, the BAO process is automated and does not require person-hour, unlike VMAT planning where planner experience in choosing the arc set-up may play an important role in plan quality.[2] Nevertheless, NC-VMAT and colli-DTRT are more complex than VMAT at the delivery stage where the risk of collision must be carefully assessed on a daily basis and patient set-up should be verified when the table is moved between arcs.

Other groups have investigated the use of non-coplanar partial arcs to treat skull-based targets. MacDonald et al. developed CODA where collimator angle is static but optimized for each partial non-coplanar arc.[3] Their BAO method considers geometric overlap metrics to choose the table angles and the gantry angle range, similar to our geometric approach for colli-DTRT.[18] This

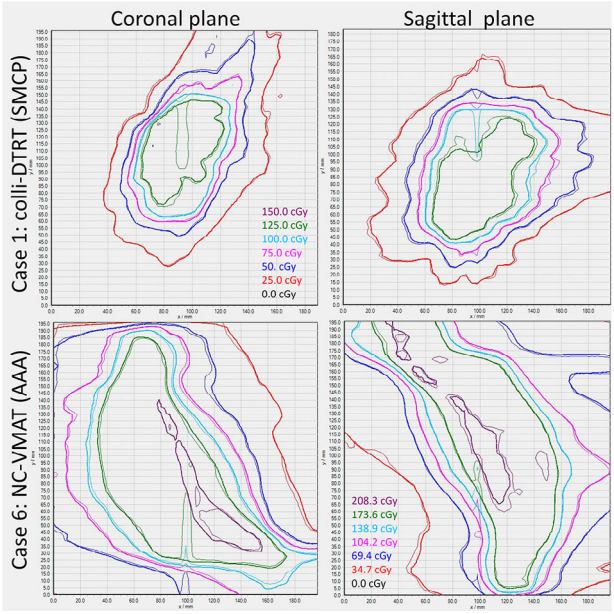

FIGURE 9 Comparison between measured dose (thin lines) and calculated dose (thick line) for the colli-DTRT plan of case 1 (top) and the NC-VMAT of case 6 (bottom).

approach was also used for a planning study of ventricular tachycardia,[17] showing applicability in the thorax. For lung cases, the authors introduced a sampling score to maintain conformity[33]; with dosimetrically motivated BAO as in our study, this was not needed. Wild et al. used optimized multiple great circles around the patient to solve the BAO problem for nasopharyngeal cases but they did not consider the use of partial arcs.[4] Partial arcs are an advantage for non-coplanar techniques owing to a reduced collision risk, especially for treatment sites in the body. However, this also introduces a new degree of freedom for the BAO process to solve: determining start and stop angles for each arc. In our study, the thresholding step means that map points anywhere in the map can be eliminated, while in subsequent beam elimination steps, called trimming, only the edges of arc candidates are eliminable to preserve arc connectedness.

Additional degrees of freedom could be explored with conventional linacs, for example, by enabling dynamic table rotation[6–9,32,34,35] or translations.[24] However, these techniques are more complex than colli-DTRT or NC-VMAT and have so far either used geometric heuristics for path determination,[8,9,24,34,35] or they have not been shown to be deliverable.[6,7,32]

In addition to mechanical degrees of freedom (dynamic table rotation or translation, dynamic collimator rotation), electrons of different energies are also available on conventional linacs. With simultaneous optimization of photon and electron contribution,[36,37] candidate electron beam directions for multiple energies could be considered in addition to the photon candidates and beam elimination could be based on simultaneous optimization of both particles.

We demonstrated deliverability for one colli-DTRT plan with dosimetrically motivated BAO on the TrueBeam with a high dosimetric accuracy. In addition, we demonstrated feasibility of optimizing and delivering NC-VMAT plans using clinical tools. Hence, NC-VMAT represents an interesting alternative for dosimetrically motivated BAO non-coplanar techniques that could be implemented in the clinic with minimal effort using readily available hardware and software.

5 | CONCLUSIONS

We developed a dosimetrically motivated BAO for colli-DTRT and NC-VMAT treatment planning which is applicable to multiple treatment sites. On seven clinically motivated cases, colli-DTRT and NC-VMAT showed equivalent or improved results for the majority of DVH criteria. This study lays the foundation for further investigations with larger cohorts of clinically motivated cases. Deliverability of colli-DTRT in developer mode was demonstrated for one case with a high dosimetric accuracy. Furthermore, the dosimetrically motivated BAO for NC-VMAT can be used to optimize and deliver NC-VMAT plans using clinical software and delivery mode.

ACKNOWLEDGMENTS

This work was partially supported by Varian, a Siemens Healthineers Company, and grant 200021_185366 of the Swiss National Science Foundation. Calculations were performed on UBELIX (http://www.id.unibe.ch/hpc), the HPC cluster at the University of Bern.

CONFLICT OF INTEREST STATEMENT

In his role as deputy editor for Medical Physics, author M.K.F. was blinded to the review process and had no role in decisions pertaining to this manuscript.

REFERENCES

1. Bortfeld T, Schlegel W. Optimization of beam orientations in radiation therapy: some theoretical considerations. *Phys Med Biol*. 1993;38(2):291-304. doi:10.1088/0031-9155/38/2/006
2. Teoh M, Clark CH, Wood K, Whitaker S, Nisbet A. Volumetric modulated arc therapy: a review of current literature and clinical use in practice. *Br J Radiol*. 2011;84(1007):967-996. doi:10.1259/bjr/22373346
3. MacDonald RL, Syme A, Little B, Ward L, Thomas CG. Toward the combined optimization of dynamic axes (CODA) for stereotactic radiotherapy and radiosurgery using fixed couch trajectories. *Med Phys*. 2020;47(2):307-316. doi:10.1002/mp.13887
4. Wild E, Bangert M, Nill S, Oelfke U. Noncoplanar VMAT for nasopharyngeal tumors: plan quality versus treatment time. *Med Phys*. 2015;42(5):2157-2168. doi:10.1118/1.4914863
5. Smyth G, Evans PM, Bamber JC, Bedford JL. Recent developments in non-coplanar radiotherapy. *Br J Radiol*. 2019;92(1097):20180908. doi:10.1259/bjr.20180908
6. Langhans M, Unkelbach J, Bortfeld T, Craft D. Optimizing highly noncoplanar VMAT trajectories: the NoVo method. *Phys Med Biol*. 2018;63(2). doi:10.1088/1361-6560/aaa36d

7. Mullins J, Renaud MA, Serban M, Seuntjens J. Simultaneous trajectory generation and volumetric modulated arc therapy optimization. *Med Phys*. 2020;47(7):3078-3090. doi:10.1002/mp.14155
8. Fix MK, Frei D, Volken W, et al. Part 1: optimization and evaluation of dynamic trajectory radiotherapy. *Med Phys*. 2018;45(9):4201-4212. doi:10.1002/mp.13086
9. Bertholet J, Mackeprang PH, Mueller S, et al. Organ-at-risk sparing with dynamic trajectory radiotherapy for head and neck cancer: comparison with volumetric arc therapy on a publicly available library of cases. *Radiation Oncology*. 2022;17(1):122. doi:10.1186/s13014-022-02092-5
10. Breedveld S, Storchi PRM, Voet PWJ, Heijmen BJM. ICycle: integrated, multicriterial beam angle, and profile optimization for generation of coplanar and noncoplanar IMRT plans. *Med Phys*. 2012;39(2):951-963. doi:10.1118/1.3676689
11. Dong P, Lee P, Ruan D, et al. 4π non-coplanar liver SBRT: a novel delivery technique. *Int J Radiat Oncol Biol Phys*. 2013;85(5):1360-1366. doi:10.1016/j.ijrobp.2012.09.028
12. Rwigema JCM, Nguyen D, Heron DE, et al. 4 pi noncoplanar stereotactic body radiation therapy for head-and-neck cancer : potential to improve tumor control and late toxicity. *Radiat Oncol Biol*. 2015;91(2):401-409. doi:10.1016/j.ijrobp.2014.09.043
13. Yu VY, Landers A, Woods K, et al. A prospective 4π radiation therapy clinical study in recurrent high-grade glioma patients. *Int J Radiat Oncol Biol Phys*. 2018;101(1):144-151. doi:10.1016/j.ijrobp.2018.01.048
14. Ohira S, Ueda Y, Akino Y, et al. HyperArc VMAT planning for single and multiple brain metastases stereotactic radiosurgery: a new treatment planning approach. *Radiat Oncol*. 2018;13(1). doi:10.1186/s13014-017-0948-z
15. Pokhrel D, Bernard ME, Johnson J, Fabian D, Kudrimoti M. HyperArc VMAT stereotactic radiotherapy for locally recurrent previously-irradiated head and neck cancers: Plan quality, treatment delivery accuracy, and efficiency. *J Appl Clin Med Phys*. 2022;23:e13561. doi:10.1002/acm2.13561
16. Ho HW, Lee SP, Lin HM, et al. Dosimetric comparison between RapidArc and HyperArc techniques in salvage stereotactic body radiation therapy for recurrent nasopharyngeal carcinoma. *Radiat Oncol*. 2020;15(1):1-11. doi:10.1186/s13014-020-01602-7
17. Reis CQM, Little B, Lee MacDonald R, Syme A, Thomas CG, Robar JL. SBRT of ventricular tachycardia using 4pi optimized trajectories. *J Appl Clin Med Phys*. 2021;22(12):72-86. doi:10.1002/acm2.13454
18. Bertholet J, Zhu C, Mackeprang PH, et al. Development of colli-dtrt: a non-coplanar intensity modulated arc therapy technique with dynamic collimator rotation. 64th AAPM Annual Meeting and Exhibition, Washington, DC, USA, 10-14, July2022. Wiley; 2022.
19. Fix MK, Manser P, Frei D, Volken W, Mini R, Born EJ. An efficient framework for photon Monte Carlo treatment planning. *Phys Med Biol*. 2007;52(19). doi:10.1088/0031-9155/52/19/N01
20. Guyer G, Mueller S, Wyss Y, et al. Technical note: a collision prediction tool using Blender. *J Appl Clin Med Phys*. 2023;24:e14165. doi:10.1002/acm2.14165
21. Kawrakow I, Fippel M. VMC++, a fast MC algorithm for radiation treatment planning. *The Use of Computers in Radiation Therapy*. Springer; 2000:126-128. doi:10.1007/978-3-642-59758-9_46
22. Mueller S, Guyer G, Volken W, et al. Efficiency enhancements of a Monte Carlo beamlet based treatment planning process: implementation and parameter study. *Phys Med Biol*. 2023;68(4). doi:10.1088/1361-6560/acb480
23. Mueller S, Guyer G, Risse T, et al. A hybrid column generation and simulated annealing algorithm for direct aperture optimization. *Phys Med Biol*. 2022;67(7):075003. doi:10.1088/1361-6560/ac58db
24. Guyer G, Mueller S, Koechli C, et al. Enabling non-isocentric dynamic trajectory radiotherapy by integration of dynamic table translations. *Phys Med Biol*. 2022;67(17):175003. doi:10.1088/1361-6560/ac840d
25. Mueller S, Volken W, Guyer G, et al. A phantom for dosimetric quality assurance of non-coplanar and mixed beam treatment techniques. 64th AAPM Annual Meeting and Exhibition. Washington, DC, USA, 10-14, July2022. Wiley; 2022.
26. Lewis D, Chan MF. Correcting lateral response artifacts from flatbed scanners for radiochromic film dosimetry. *Med Phys*. 2015;42(1):416-429. doi:10.1118/1.4903758
27. Micke A, Lewis DF, Yu X. Multichannel film dosimetry with nonuniformity correction. *Med Phys*. 2011;38(5):2523-2534. doi:10.1118/1.3576105
28. Lewis D, Micke A, Yu X, Chan MF. An efficient protocol for radiochromic film dosimetry combining calibration and measurement in a single scan. *Medical*. 2012;39(10):6339-6350.
29. Low DA, Harms WB, Mutic S, Purdy JA. A technique for the quantitative evaluation of dose distributions. *Med Phys*. 1998;25(5):656-661. doi:10.1118/1.598248
30. Miften M, Olch A, Mihailidis D, et al. Tolerance limits and methodologies for IMRT measurement-based verification QA: recommendations of AAPM Task Group No. 218. *Med Phys*. 2018;45(4):e53-e83. doi:10.1002/mp.12810
31. Paddick I. A simple scoring ratio to index the conformity of radiosurgical treatment plans. Technical note. *J Neurosurg*. 2000;93(3):219-222. doi: 10.3171/jns.2000.93.supplement.3.0219
32. Lyu Q, Yu VY, Ruan D, Neph R, O'Connor D, Sheng K. A novel optimization framework for VMAT with dynamic gantry couch rotation. *Phys Med Biol*. 2018;63(12):125013. doi:10.1088/1361-6560/aac704
33. Lincoln JD, MacDonald RL, Syme A, Thomas CG. Static couch non-coplanar arc selection optimization for lung SBRT treatment planning. *Phys Med Biol*. 2023;68(15):155011. doi:10.1088/1361-6560/ace23f
34. Smyth G, Evans PM, Bamber JC, et al. Dosimetric accuracy of dynamic couch rotation during volumetric modulated arc therapy (DCR- VMAT) for primary brain tumours. *Phys Med Biol*. 2019;64.
35. Yang Y, Zhang P, Happersett L, et al. Choreographing couch and collimator in volumetric modulated arc therapy. *Int J Radiat Oncol Biol Phys*. 2011;80(4):1238-1247. doi:10.1016/j.ijrobp.2010.10.016
36. Mueller S, Fix MK, Joosten A, et al. Simultaneous optimization of photons and electrons for mixed beam radiotherapy. *Phys Med Biol*. 2017;62(14):5840-5860. doi:10.1088/1361-6560/aa70c5
37. Mueller S, Manser P, Volken W, et al. Part 2: dynamic mixed beam radiotherapy (DYMBER): photon dynamic trajectories combined with modulated electron beams. *Med Phys*. 2018;45(9):4213-4226. doi:10.1002/mp.13085

SUPPORTING INFORMATION

Additional supporting information can be found online in the Supporting Information section at the end of this article.

How to cite this article: Bertholet J, Zhu C, Guyer G, et al. Dosimetrically motivated beam-angle optimization for non-coplanar arc radiotherapy with and without dynamic collimator rotation. *Med Phys*. 2023;1-14. https://doi.org/10.1002/mp.16899